# Biospecific Affinity Chromatography: Computational Modelling *via* Lattice Boltzmann Method and Influence of Lattice-Based Dimensionless Parameters

Dayane C.G. Okiyama, Eliana S. Kamimura and José A. Rabi*

*Faculty of Animal Science and Food Engineering, University of São Paulo Av. Duque de Caxias Norte 225, Pirassununga, SP, 13635-900, Brazil*

**Abstract:** Based on a dynamic (i.e. time-dependent) one-dimensional approach, this work applied lattice Boltzmann method (LBM) to computationally model biospecific affinity chromatography (BAC). With governing equations expressed in lattice-based dimensionless form, LBM was implemented in D1Q2 lattice by assigning particle distribution functions to adsorbate concentration in both fluid and solid phases. The LBM simulator was firstly tested in view of a classic BAC work on lysozyme and the streaming step relating to adsorbate concentration in the solid-phase was suppressed from the LBM code with no loss of functionality. Expected behaviour of breakthrough curves was numerically reproduced and the influence of lattice-based dimensionless parameters was examined. The LBM simulator was next applied so as to assess lattice-based dimensionless parameters regarding an experimental BAC work on lipase.

**Keywords:** Biospecific affinity chromatography, phenomenological modelling, numerical simulation, lattice Boltzmann method.

## 1. INTRODUCTION

Innovative design, scale-up procedures and optimal operation can be rapidly achieved *via* numerical simulation [1], thus reducing the number of tests and saving valuable material and human resources required in bioseparation processes. Given the costs of industrial-scale experimentation, distinct design parameters and operation scenarios can be numerically tested for process viability [2] and such has been the case of bioreactor engineering [3-5].

Bioseparation models are prone to be complex enough to justify computational modelling [6-8] and biospecific affinity chromatography (BAC) may benefit from it if comprehensive knowledge is required [9]. Use of computational fluid dynamics (CFD) towards bioprocesses has increased as its importance has been recognized while suitable techniques have been developed [10].

Distinct approaches can be followed. By relying on continuum concept, macroscale simulation applies basic conservation principles to obtain differential equations to observable properties, which are numerically solved. Finite differences method (FDM), finite elements method (FEM) and finite volumes method (FVM) have been among widespread discretization techniques for food and bioprocesses [11-16].

Microscale models individually identify constituent particles in conjunction with their mutual interactions. In molecular dynamics (MD) simulation, Newtonian mechanics is then applied to predict space-time evolution of such (colossal!) particle collection while statistical mechanics is applied to retrieve observable properties. The task is to simulate macroscopic behaviour from microscopic modelling, requiring huge computational effort and memory resources. MD has been used in pharmacological and emulsion research [17-20].

Between those two scales, mesoscopic models treat bulk media as cellular automata, i.e. as systems where quantities may only assume discrete values [21]. From the mathematical viewpoint, a particle distribution function is introduced in order to describe the behaviour of constituent particle collections [22]. Based on that function one implements lattice Boltzmann method (LBM), regarded as an extension of its predecessor method, namely lattice-gas cellular automata [23].

With pioneering ideas launched in [24] and more recent if compared to long-standing methods (e.g. FDM, FEM or FVM), LBM has become an alternative technique to simulate food and bioprocesses [25]. Interesting applications in view of biosystems have comprised flow through fibrous materials [26], particle suspensions and particle-fluid interactions [27], solute transport in porous media [28, 29], fluid dynamics of blood [30, 31], liquid-vapour interface [32] and chromatography [33, 34].

*Address correspondence to this author at the Faculty of Animal Science and Food Engineering, University of São Paulo Av. Duque de Caxias Norte 225, Pirassununga, SP, 13635-900, Brazil; Tel: +55 19 35654257;
Fax: +55 19 35656865; E-mail: jrabi@usp.br

ISSN: 1927-3037/15 

As part of on-going research on LBM simulation of food and bioprocesses [35], LBM has been applied to biospecific affinity chromatography (BAC). Based on a dynamic one-dimensional reaction-diffusive model with Langmuir kinetics [36, 37], this work aimed at the computational modelling of one-component breakthrough curves *via* LBM. Governing differential equations were cast in lattice-based dimensionless form together with initial and boundary conditions. Trial LBM simulations were performed in view of a classic BAC work on lysozyme [38] and the LBM simulator was next applied towards an existing experimental work on lipase bioseparation [39].

While there is no doubt about the efficiency of methods like FDM, FEM or FVM to perform equivalent simulations, comparisons in terms of computational effort and memory use fall beyond the purpose of this work. Rather, its goal is to present LBM as an alternative route for BAC simulation. By rendering relatively simpler codes [40], LBM can easily deal with moving or free boundaries while being able to simulate fluid flow without directly solving Navier-Stokes equations. Such features are particularly appealing for those who have programmed their own computational fluid dynamics codes *via* FDM, FEM or FVM.

## 2. THEORY

### 2.1. Mathematical Models for Biospecific Affinity Chromatography (BAC)

BAC models have typically invoked 2nd-order adsorption and 1st-order desorption kinetics, uniform fluid flow and adsorbate transport by either convection or diffusion [7, 9, 16, 38, 41-43]. Additional assumptions have included uniform porosity $\varepsilon$ over the chromatographic column and constant volumetric flow rate $\dot{V}$ of the percolating solution. Hence, interstitial fluid velocity $v = \dot{V}/(\varepsilon A)$ results uniform, being $A$ the cross-sectional area of the column. In model equations one may use superficial velocity $\bar{v} = \dot{V}/A$, also referred to as seepage velocity, which is related to interstitial velocity *via* Dupuit-Forchheimer relation $\bar{v} = \varepsilon v$ [44]. Those models are dynamic with 1st-order spatial dependence so that adsorbate concentrations are allowed to vary along a coordinate $z$ (usually the column axis) besides depending on time $t$.

This work modelled chromatographic columns as stratified cylindrical fixed-beds with inlet at $z = 0$ and outlet at $z = L$ (= column length). Adsorbate concentrations in fluid and solid phases were identified respectively as $c = c(z,t)$ and $q = q(z,t)$ while corresponding governing partial differential equations (PDEs) were put forward as:

$$\frac{\partial c}{\partial t} + v\frac{\partial c}{\partial z} = D\frac{\partial^2 c}{\partial z^2} - \frac{1-\varepsilon}{\varepsilon}\dot{r} \tag{1}$$

$$\dot{r} = \frac{\partial q}{\partial t} = k_{\text{ads}}c(q_{\max} - q) - k_{\text{des}}q \tag{2}$$

where $D$ is axial diffusivity in the fluid phase, $\dot{r}$ is the instantaneous rate at which adsorbate is transferred from fluid to solid phase, $k_{\text{ads}}$ and $k_{\text{des}}$ are respectively adsorption and desorption coefficients, and $q_{\max}$ is the maximum adsorption capacity (i.e. saturation) of the column.

Initial conditions were prescribed as:

$$c(z,0) = 0 \text{ and } q(z,0) = 0 \text{ , for } 0 \le z \le L \tag{3}$$

In the proposed model framework, the governing equation for solid-phase concentration lacks partial derivatives with respect to coordinate $z$ so that boundary conditions were only required for the fluid-phase PDE. Being $c_{\text{in}} \neq 0$ the adsorbate concentration in feed solution, one may impose Dirichlet condition at column inlet ($z = 0$) [7, 41, 45] and null Neumann condition at column exit ($z = L$), namely:

$$c(0,t) = c_{\text{in}} \text{ and } \left.\frac{\partial c}{\partial z}\right|_{z=L} = 0 \text{ , for } t > 0 \tag{4}$$

At inlet, one may alternatively prescribe Danckwerts condition [16, 34, 42], namely:

$$v c_{\text{in}} = v c(0,t) - D\left.\frac{\partial c}{\partial z}\right|_{z=0} \text{ , for } t > 0 \tag{5}$$

which simplifies to Dirichlet condition if $D = 0$.

In this work, LBM simulations use process parameters as suggested in [41], where Dirichlet inlet condition is adopted (thus Danckwerts condition was disregarded). Moreover, a numerical study has shown that no practical effect is introduced when one boundary condition is replaced by the other for low mass diffusivities, $D < 10^{-8}$ m$^2$/s [46]. Differences become noticeable for $D > 10^{-8}$ m$^2$/s but, in this case, simulated breakthrough curves deviate from experimental data, regardless of the boundary condition type imposed at column inlet.

### 2.2. Rationale of Lattice-Boltzmann Method (LBM)

Inspired on kinetic gas theory, LBM is a bottom-up technique different not only from top-down methods like

FDM, FEM or FVM but also from MD simulation, which is another bottom-up approach [22]. Contrast from MD relies on the fact that LBM treats the macroscale medium, whether solid or fluid, as a set of fictitious particles in a discrete space, namely a fictitious lattice. During discrete time steps and according to their speeds, such particles travel (stream) between adjacent sites along pre-defined directions (lattice links). As particles arrive at lattice sites, they mutually collide and their velocities become rearranged. By imposing mass and momentum conservations to such dynamics, referred to as streaming and collision, macroscopic behaviour can be simulated [23].

LBM mathematically relies on a particle distribution function $f(\vec{r},\vec{u},t)$ giving the probability of finding, at time $t$, fictitious particles about position $\vec{r}$ with velocities between $\vec{u}$ and $\vec{u}+\mathrm{d}\vec{u}$. Observable properties (e.g. species concentration, bulk flow velocity or temperature) can be retrieved through moments of function $f$ [25, 40].

LBM is implemented to numerically obtain function $f$, which is ruled by Boltzmann transport equation. In the absence of external forces, such governing equation is written as:

$$\frac{\partial f}{\partial t}+\vec{u}\cdot\vec{\nabla}f=\Omega(f) \xrightarrow{\text{BGK approximation for }\Omega} \frac{\partial f}{\partial t}+\vec{u}\cdot\vec{\nabla}f=\frac{f^{\mathrm{eq}}-f}{\Delta t_{\mathrm{relax}}} \tag{6}$$

where the collision operator $\Omega = \Omega(f)$ gives the variation rate of function $f$ due to collisions between particles. In Equation (6), BGK approximation (after Bhatnagar-Gross-Krook) has been invoked to linearize such operator as $\Omega(f) = (f^{eq} - f)/\Delta t_{relax}$ [47], meaning that particles tend to local equilibrium values $f^{eq}$ at a rate controlled by a relaxation time $\Delta t_{relax}$ [48, 49].

In LBM, Equation (6) is written for each link $k$ in the fictitious lattice so that it becomes referred to as lattice-Boltzmann equation:

$$\frac{\partial f_k}{\partial t}+\vec{u}_k\cdot\vec{\nabla}f_k=\frac{f_k^{\mathrm{eq}}-f_k}{\Delta t_{\mathrm{relax}}} \tag{7}$$

Distinct lattices are identified as D$n$Q$m$, where $n$ is the problem dimensionality (e.g., $n$ = 1 = 1-D = one dimensional) and $m$ refers to the speed model (= number of particle distribution functions to be solved for each observable property). Typical lattices for LBM simulations are depicted elsewhere [23, 25, 40].

Space-time discretisation of Equation (7) written for a given macroscopic property yields an algebraic equation whose numerical evolution is accomplished in two steps. During collision (time evolution), particle distribution functions $f_k$ are updated from instant $t$ to $t + \Delta t$ at all lattice sites, being $\Delta t$ the advancing time step. During streaming (spatial evolution), collision updates are transferred to adjacent sites.

The connection between mesoscale (LBM simulation) and macroscale (observable properties) is established by means of the equilibrium distribution function $f^{eq}$ together with the relaxation parameter $\omega = \Delta t_{relax}/\Delta t$. The former dictates the transport phenomenon (i.e. momentum, heat or mass transfer) while the later sets the related transport coefficient (i.e. kinematic viscosity, thermal diffusivity or mass diffusivity).

## 3. NUMERICAL METHOD

### 3.1. BAC Model Equations in Lattice-Based Dimensionless Form

The BAC model described in section 2.1 was cast in dimensionless form as an attempt to deal with concurrent effects while aiming at fewer parameters. Being $\dot{r}_{\mathrm{ref}} \neq 0$ a reference value for adsorbate transfer rate defined ahead, dimensionless variables were based on LBM parameters $\Delta z$ and $\Delta t$ as well as on BAC parameters $c_{in}$ and $q_{max}$ as follows:

$$Z=\frac{z}{\Delta z}\quad,\quad \tau=\frac{t}{\Delta t}\quad,\quad C=\frac{c}{c_{\mathrm{in}}}\quad,\quad Q=\frac{q}{q_{\max}}\quad,\quad \dot{R}=\frac{\dot{r}}{\dot{r}_{\mathrm{ref}}} \tag{8}$$

Accordingly, lattice-based dimensionless forms of Equations (1) and (2) resulted as:

$$\frac{\partial C}{\partial \tau}+\mathrm{Ma}\frac{\partial C}{\partial Z}=\frac{1}{\mathrm{Pe_m}}\frac{\partial^2 C}{\partial Z^2}-\frac{1-\varepsilon}{\varepsilon}P_{\max}\dot{R} \tag{9}$$

$$\dot{R}=\frac{\partial Q}{\partial \tau}=P_{\mathrm{ads}}C(1-Q)-P_{\mathrm{des}}Q \tag{10}$$

Lattice-based Mach number (Ma) and mass-transfer Peclet number ($\mathrm{Pe_m}$) were defined as:

$$\mathrm{Ma}=\frac{v\Delta t}{\Delta z}\quad\text{and}\quad \mathrm{Pe_m}=\frac{(\Delta z)^2}{D\Delta t} \tag{11}$$

By identifying $\dot{R}=\partial Q/\partial\tau$ as claimed in Equation (10), reference value for adsorbate transfer rate

resulted as $\dot{r}_{\text{ref}} = q_{\max}/\Delta t$ so that the remaining dimensionless parameters became:

$$P_{\max} = \frac{\dot{r}_{\text{ref}}\,\Delta t}{c_{\text{in}}} = \frac{q_{\max}}{c_{\text{in}}} \quad , \quad P_{\text{ads}} = k_{\text{ads}}\, c_{\text{in}}\, \Delta t \quad , \quad P_{\text{des}} = k_{\text{des}}\, \Delta t \quad (12)$$

By introducing $N_z = L/\Delta z$ so that $N_z + 1$ is the number of lattice sites in $z$ axis including end points, initial and boundary conditions, Equations (3) and (4), respectively became:

$$C(Z,0) = 0 \text{ and } Q(Z,0) = 0 \text{ , for } 0 \le Z \le N_z \quad (13)$$

$$C(0,\tau) = 1 \text{ and } \left.\frac{\partial C}{\partial Z}\right|_{Z=N_z} = 0 \text{ , for } \tau > 0 \quad (14)$$

### 3.2. LBM Implementation for BAC Simulation

Based on BGK approach, LBM was programmed in Fortran 90/95 to simulate BAC ruled by Equations (9) to (14), with code lines following [40]. As the proposed model deals with adsorbate concentrations in fluid and solid phases, two particle distribution functions were required. Functions $f_k = f_k(Z,\tau)$ were assigned to dimensionless fluid-phase concentration $C = C(Z,\tau)$ whereas functions $s_k = s_k(Z,\tau)$ referred to solid-phase counterpart $Q = Q(Z,\tau)$.

At any dimensionless instant $\tau$ and position $Z$ within the chromatographic column, dimensionless adsorbate concentrations were retrieved as:

$$C(Z,\tau) = f_1(Z,\tau) + f_2(Z,\tau) \text{ and } Q(Z,\tau) = s_1(Z,\tau) + s_2(Z,\tau) \quad (15)$$

where $k = 1$ and $k = 2$ refer to forward and backward streaming directions, respectively. LBM was implemented in D1Q2 lattice so that functions $f_0$ and $s_0$ were disregarded.

The underlying physics at each phase dictates the equilibrium distribution functions $f_k^{\text{eq}}$ and $s_k^{\text{eq}}$ as well as the relaxation factors $\omega_f$ and $\omega_s$. Provided that the solid matrix remains stationary while diffusive-convective transport takes place in the fluid phase, the equilibrium distribution functions were adopted as [40]:

$$f_k^{\text{eq}}(Z,\tau) = w_k\, C(Z,\tau)\, [1 \pm \text{Ma}] \quad \text{and} \quad s_k^{\text{eq}}(Z,\tau) = w_k\, Q(Z,\tau) \quad (16)$$

Fulfilling the condition $\sum w_k = 1$, weighting factors $w_k$ are the same for $f_k^{\text{eq}}$ and $s_k^{\text{eq}}$, namely $w_0 = 0$ (i.e. $f_0$ and $s_0$ are disregarded) and $w_1 = w_2 = 1/2$ for D1Q2 lattice. The sign before Mach number depends on streaming direction, being +Ma for forward ($k = 1$) and –Ma for backward ($k = 2$) streaming.

For governing equations invoking diffusive mass transport, relaxation factor $\omega$ refers to diffusivity $D$. Consistent with $\text{Pe}_m$ definition in Equation (11), the following expressions were applied [35]:

$$\omega_f = \left(\frac{1}{\text{Pe}_m} + \frac{1}{2}\right)^{-1} \text{ and } \omega_s = 2 \quad (17)$$

In LBM, eventual source or sink terms are introduced in the collision step [40]. In view of Equations (9) and (10), the following expressions were computationally implemented:

$$f_k(Z,\tau+\Delta\tau) = [1-\omega_f]\, f_k(Z,\tau) + \omega_f\, f_k^{\text{eq}}(Z,\tau) - w_k\left(\tfrac{1-\varepsilon}{\varepsilon} P_{\max}\dot{R}\right)\Delta\tau \quad (18)$$

$$s_k(Z,\tau+\Delta\tau) = [1-\omega_s]\, s_k(Z,\tau) + \omega_s s_k^{\text{eq}}(Z,\tau) + w_k\, \dot{R}\,\Delta\tau \quad (19)$$

where $\Delta\tau$ is the dimensionless time step and $\dot{R} = P_{\text{ads}}\, C\,(1-Q) - P_{\text{des}}\, Q$.

At this point, it is worth recalling the absence of partial derivatives with respect to coordinate $Z$ in Equation (10). As far as the streaming step is concerned in such a case, one may implement LBM by either imposing periodic boundary conditions or simply suppressing the streaming step itself [50]. The later approach was adopted so that streaming was solely implemented for fluid-phase particle distribution functions as:

$$f_k(Z+\Delta Z_k,\tau+\Delta\tau) = f_k(Z,\tau+\Delta\tau) \quad (21)$$

being $\Delta Z_k$ the dimensionless separation distances between lattice sites. Yet, systems modeled by zero-order equations with respect to space may still "perceive" external influence through source and/or sink terms [35].

With $C(Z,0)$ and $Q(Z,0)$ provided by Equation (13), initial conditions for particle distribution functions were imposed as:

$$f_k(Z,0) = w_k\, C(Z,0) \text{ and } s_k(Z,0) = w_k\, Q(Z,0) \quad (21)$$

At inlet ($Z = 0$), $f_2(0,\tau)$ was obtained *via* streaming from the adjacent site at $Z = 1$ so that $f_1(0,\tau)$ was the only unknown. As Equation (14) provides $C(0,\tau) = 1$, flux conservation leads to the following condition [40]:

$$f_1(0,\tau) = C(0,\tau) - f_2(0,\tau) \quad \Rightarrow \quad f_1(0,\tau) = 1 - f_2(0,\tau) \qquad (22)$$

At outlet ($Z = N_z$), $f_1(N_z,\tau)$ was obtained *via* streaming from the adjacent site at $Z = N_z - 1$ so that $f_2(N_z,\tau)$ was unknown. By approximating the null Neumann condition in Equation (14) by first-order finite-differences [40], the following condition was obtained:

$$f_2(N_z,\tau) = f_2(N_z - 1,\tau) \qquad (23)$$

## 4. RESULTS AND DISCUSSION

### 4.1. Trial LBM Simulations Against a Classic BAC Work

Implementation of the LBM simulator was tested against a classic work on lysozyme bioseparation [38], whose parameters concerning a given chromatographic column are shown in Table **1a** together with LBM parameters $\Delta z$ and $\Delta t$. The later were adopted so as to ensure low lattice-based Mach number [40] whereas the former were used in simulations performed in [41]. Bed porosity was set as $\varepsilon = 0.5$ so that Equations (1) and (2) could match model equations in [41] as $(1 - \varepsilon)/\varepsilon = 1$. For LBM simulations, Table **1b** shows lattice-based dimensionless parameters obtained by means of Equations (11) and (12).

**Table 1 (a) Process Parameters Concerning Lysozyme Bioseparation [38] and LBM Parameters $\Delta z$ and $\Delta t$, (b) Resulting Lattice-Based Dimensionless Parameters for LBM Simulations**

| (a) BAC and LBM parameters | (b) Lattice-based dimensionless parameters |
|---|---|
| $L = 0.104$ m | $N_z = 1040$ |
| $c_{in} = 0.0071$ mol/m$^3$ | $P_{max} = 123.24$ |
| $q_{max} = 0.875$ mol/m$^3$ | $P_{ads} = 1.0153 \times 10^{-4}$ |
| $k_{ads} = 0.286$ m$^3$/(mol·s) | $P_{des} = 2.5 \times 10^{-5}$ |
| $k_{des} = 0.0005$ s$^{-1}$ | Ma = 0.112 |
| $v = 0.000224$ m/s | $\Delta Z = 1$ |
| $\Delta z = 0.0001$ m | $\Delta\tau = 1$ |
| $\Delta t = 0.05$ s | |

For comprehensiveness towards large-scale BAC, axial diffusion was considered in the fluid phase. Functionality of the LBM simulator was tested for distinct lattice-based mass-transfer Peclet numbers, namely $Pe_m = 0.15$, 0.30, 1.00 and $\infty$, the latter being implemented by setting $\omega_f = 2$ in agreement with Equation (17). For each testing $Pe_m$, Figure **1a** compares experimental data [38] with breakthrough curves $C_{exit}(\tau) = C(N_z,\tau)$ simulated using parameters from Table **1**.

Despite breakthrough curves are shifted to right with respect to time, their expected shape was reproduced. It is worth noting that curve slope reduces as $Pe_m$ decreases, i.e. as mass diffusion becomes more influential. This is because diffusion "spreads" species to both forward and backward directions in 1-D transport. Hence, saturation front becomes smoother than if transported solely by convection.

Additional simulations were performed in [41] by adopting a slightly lower maximum adsorption capacity, namely $q'_{max} = 0.845$ mol/m$^3$, for which Equation (12) provides $P'_{max} = 119.01$. For each trial $Pe_m$ as in prior LBM simulations, Figure **1b** shows that numerically simulated breakthrough curves are closer to experimental data, i.e. saturation arrives earlier at the column exit as expected. Moreover, as parameters $Pe_m$ were kept the same, the slope of each corresponding breakthrough curve remains apparently unchanged.

With regard to the original $q_{max}$ value, two lower maximum adsorption capacities were tested, namely $q''_{max} = 0.95\,q_{max}$ and $q'''_{max} = 0.90\,q_{max}$, respectively rendering $P''_{max} = 117.08$ and $P'''_{max} = 110.92$. By keeping $Pe_m = 0.30$ (as this value yields a slope close to experimental data), Figure **1c** shows the corresponding simulated breakthrough curves, where good match is observed for $P''_{max} = 117.08$.

It is worth mentioning that some simulations were carried out in [41] by disregarding diffusive transport in fluid phase, which is mathematically equivalent to assume $D = 0$ in Equation (1) or $Pe_m \to \infty$ in Equation (9). In this case, fluid-phase concentration becomes ruled by a first-order PDE with respect to spatial dependence and adsorbate transport in fluid phase becomes convection-dominant. In doing so, one may claim the advantage of being able to apply marching numerical methods for initial-value problems (e.g., Runge-Kutta method) while dismissing the additional boundary condition at column exit.

Nonetheless, discretisation schemes of convective terms (e.g. upwind scheme) might yield numerical dispersion [51], also referred to as false diffusion, which is not the case of LBM [25, 40]. In FDM, for instance, numerical dispersion due to upwind schemes becomes evident for convection prevailing over diffusion [52], i.e. for higher $Pe_m$. For that reason, slope of breakthrough curves simulated in [41] with parameters from Table **1a** could be "artificially

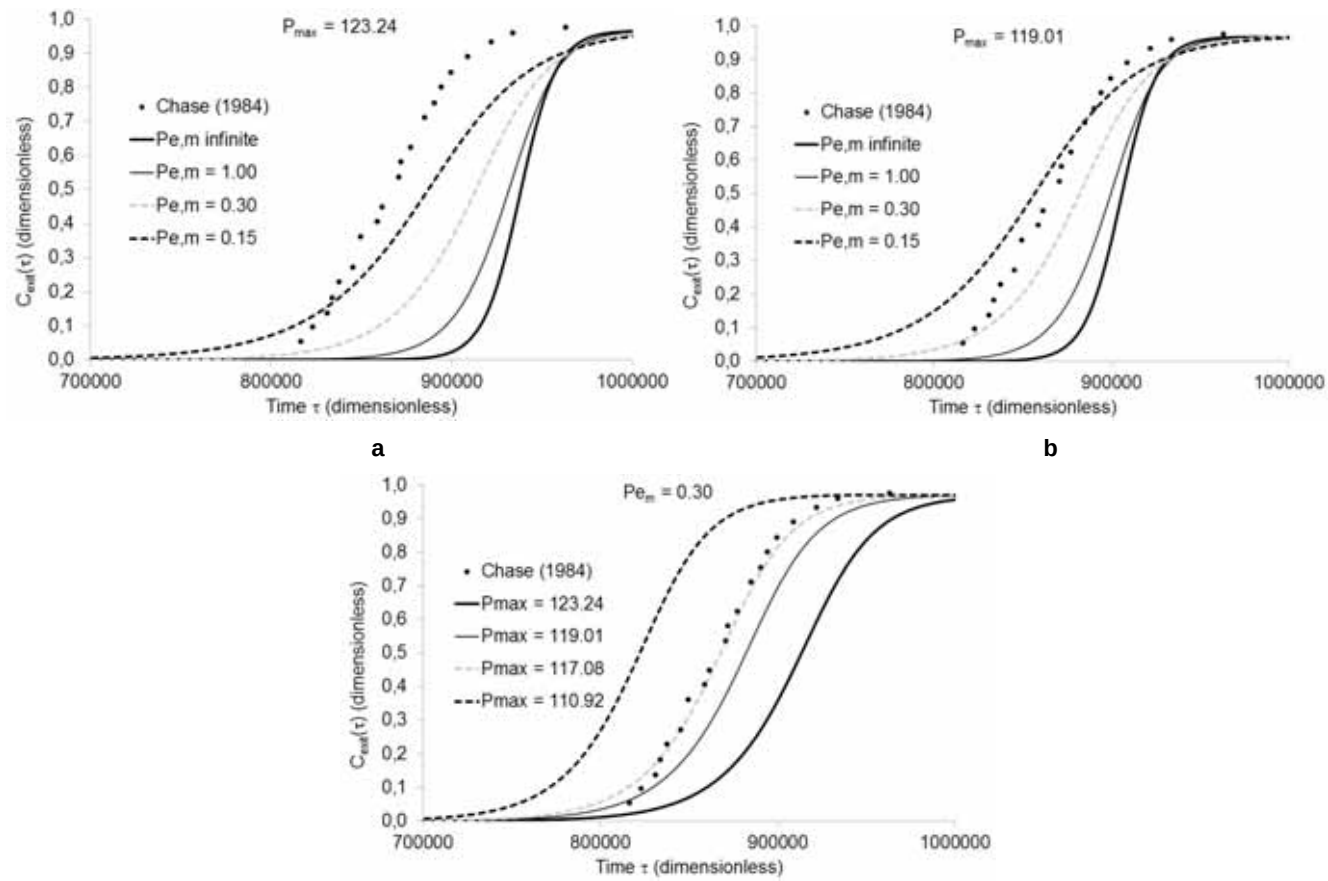


**Figure 1:** Comparison between experimental data [38] and breakthrough curves simulated with lattice-based dimensionless parameters as assessed from (**a**) model parameters in [41] and distinct mass-transfer Peclet numbers $Pe_m$, (**b**) lower maximum adsorption capacity as suggested in [41] and distinct mass-transfer Peclet numbers $Pe_m$, (**c**) trial higher values of maximum adsorption capacity and $Pe_m = 0.30$.

smoother", which may suggest a re-evaluation of some (if not all) parameters. As depicted in Figures **1a** and **1b**, curves simulated *via* LBM with $Pe_m \to \infty$, i.e. which mimic numerical simulations in [41], seem steeper than experimental data.

### 4.2. LBM Simulation of BAC for Lipase Bioseparation

Thanks to industrial and medical applications, there has been a growing interest in microbial lipases, whose high-degree purification can be achieved through BAC [53]. After trial tests as addressed in section 4.1, the LBM simulator was applied to lipase bioseparation. Along with LBM parameters $\Delta z$ and $\Delta t$, Table **2a** shows parameters concerning a given column studied in [39]. Adsorbate concentrations are here expressed in enzymatic activity units defined as 1 U = 1 μmol of fatty acids released per minute. However, lattice-based dimensionless parameters are insensitive to units and Table **2b** shows their values as assessed by Equations (11) and (12). Bed porosity was initially set at $\varepsilon = 0.5$.

**Table 2: (a) Process Parameters Concerning Lipase Bioseparation [39] and LBM Parameters $\Delta z$ and $\Delta t$, (b) Resulting Lattice-Based Dimensionless Parameters for LBM Simulations**

| (a) BAC and LBM parameters | (b) Lattice-based dimensionless parameters |
|---|---|
| $L = 0.032$ m | |
| $c_{in} = 9.52\times10^{6}$ U/m$^3$ | $N_z = 320$ |
| $q_{max} = 9.89\times10^{7}$ U/m$^3$ | $P_{max} = 10.389$ |
| $k_{ads} = 1.00\times10^{-9}$ m$^3$/(U·s) | $P_{ads} = 4.76\times10^{-4}$ |
| $k_{des} = 0.00233$ s$^{-1}$ | $P_{des} = 1.17\times10^{-4}$ |
| $v = 0.00025$ m/s | Ma = 0.125 |
| $D = 3.06\times10^{-8}$ m$^2$/s | $Pe_m = 6.536$ |
| $\Delta z = 0.0001$ m | $\Delta Z = 1$ |
| $\Delta t = 0.05$ s | $\Delta\tau = 1$ |

Recalling that values in Table **2a** are tentative, LBM simulations were also performed for different values of dimensionless parameters $P_{max}$, $Pe_m$ and $\varepsilon$ (i.e. variations in adsorption-desorption parameters $P_{ads}$ and

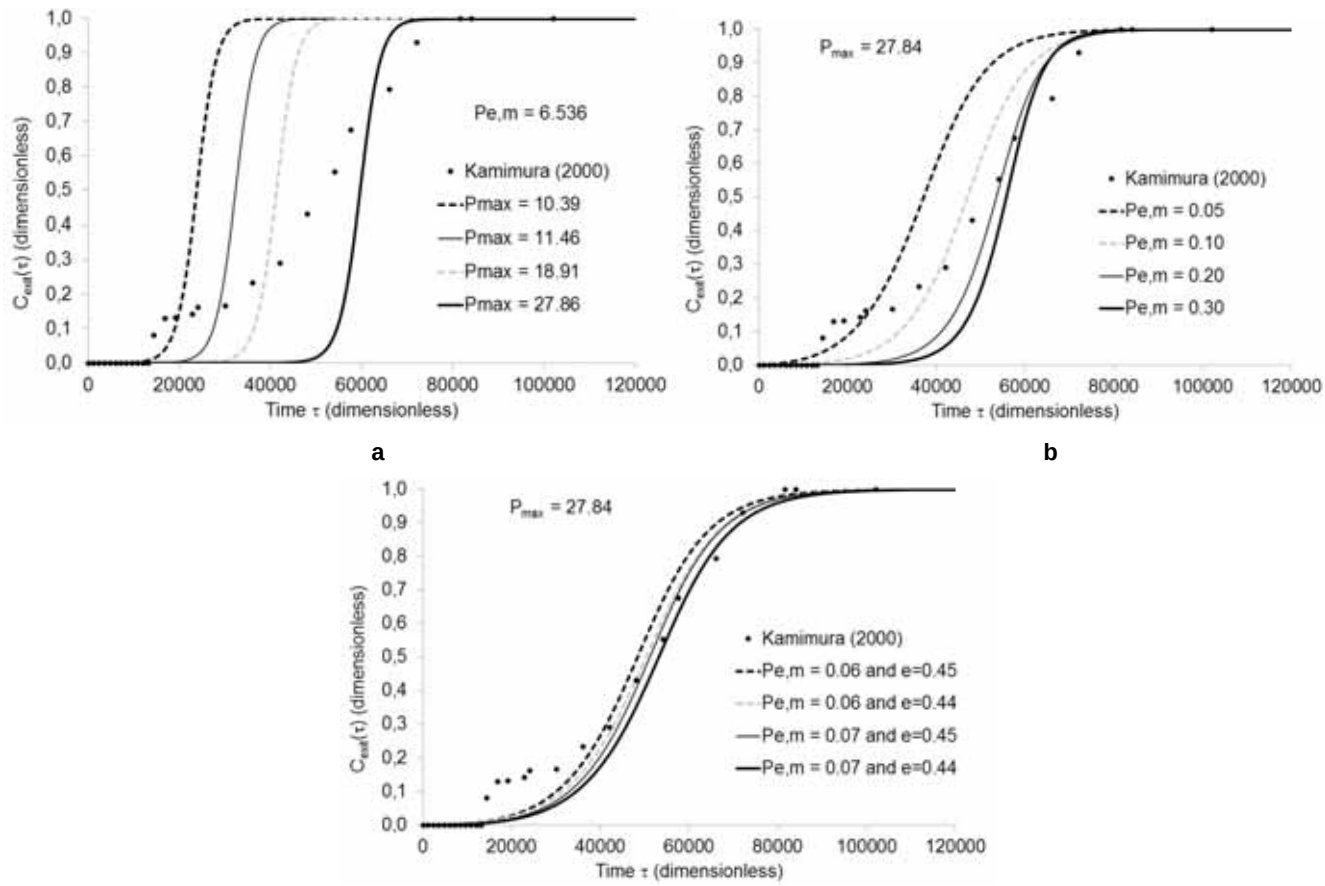


**Figure 2:** Comparison between experimental data [39] and breakthrough curves simulated with lattice-based dimensionless parameters as assessed from (**a**) distinct maximum adsorption capacities as suggested in [39] and mass-transfer Peclet number $Pe_m$ = 6.536, (**b**) the highest maximum adsorption capacity in [39] and distinct $Pe_m$, (**c**) the highest maximum adsorption capacity and combinations of $Pe_m$ = 0.06 or 0.07 with trial lower porosities ε = 0.44 or 0.45.

$P_{des}$ were not tested). In Figure **2a**, experimental data [39] are compared with breakthrough curves as simulated with parameters from Table **2b** as well as exploratory higher $P_{max}$ = 11.46, 18.91 and 27.86. Such values are related *via* Equation (12) to higher $q_{max}$ equally tested in [39]. One notes that saturation arrives at proper time at column exit but slopes need some adjustment.

Accordingly, Figure **2b** shows breakthrough curves as simulated with tentative $Pe_m$, namely 0.05, 0.10, 0.20 and 0.30, while keeping $P_{max}$ = 27.86. As expected and as pointed in section 4.1, curve slopes are reduced inasmuch as $Pe_m$ decreases. Yet, numerically simulated curves remain distant from experimental data, thus claiming for further tests.

Figure **2c** shows breakthrough curves simulated with $P_{max}$ = 27.86 while combining either $Pe_m$ = 0.06 or 0.07 with porosity ε = 0.44 or 0.45. Any combination of those values of diffusivity $D$ (for $Pe_m$ calculations) or bed porosity ε yields reasonable curves. It should be noted that experimental assessment of aforementioned parameters is not straightforward.

## 5. CONCLUSION AND FUTURE WORK

Computational modelling of biospecific affinity chromatography (BAC) requires the solution of coupled partial differential equations and lattice-Boltzmann method (LBM) comes forward as an interesting numerical technique. This work applied LBM following a dynamic one-dimensional BAC model cast in dimensionless form so that lattice-based Mach number (Ma) and mass-transfer Peclet number ($Pe_m$) arose as model parameters.

As the differential equation for adsorbate concentration in solid phase lacked partial derivatives with respect to spatial coordinate, the related streaming step was simply suppressed in the LBM code. No loss of functionality was observed as the LBM simulator was able to reproduce the expected shape of breakthrough curves.

Influence of $Pe_m$ (sometimes neglected in BAC models) and dimensionless parameter $P_{max}$ related to maximum adsorption capacity of the column was examined by performing LBM simulations of a classic work on lysozyme bioseparation. While $Pe_m$ influenced the slope of the breakthrough curve, $P_{max}$ affected the time lag for column saturation. Differences between simulated breakthrough curves and experimental data were assigned to the absence of numerical diffusion in LBM. Those discrepancies were mitigated by re-evaluating the original model parameters.

Numerical simulations of lipase bioseparation proved that bed porosity are influential in BAC models, apart from lattice-based dimensionless parameters $Pe_m$ and $P_{max}$. In view of an accurate assessment of model parameters *via* best-fit against experimental data, the numerical simulator is currently being extended in order to combine the LBM solution procedure with optimisation routines (to minimise the sum of squared differences between numerical and experimental breakthrough curves).

At its current development stage the LBM simulator is limited to 1-D modelling and extension to 2-D models implies in simulating the downstream solution as well. Accordingly, upcoming versions of the LBM simulator will cope with bed hydrodynamics by the use of D2Q9 lattices not only for flow simulation but also mass transfer as already accounted for.

The LBM simulator will be equally extended towards multi-component bioseparation. As pointed in [23], LBM may tackle multiphase flows by relying on a set of multicomponent distribution functions $f_{ki}$ with index $i$ running over as many species as necessary, e.g. other enzymes or protein products. In view of that, corresponding adsorption-desorption kinetics should be properly modelled and numerically implemented *via* source or sink terms $R_{ki}$ related to the variation rate of species $i$ for each lattice link $k$.

## ACKNOWLEDGEMENTS

Authors thank FAPESP (São Paulo Research Foundation, Brazil) for the financial support to research projects 2005/02538-1 and 2012/23459-6, from which the present work derives.

## APPENDIX: NOMENCLATURE

### Latin Symbols

$A$ = cross-sectional area of the chromatographic column, $m^2$

$C$ = dimensionless adsorbate concentration in fluid phase

$c$ = adsorbate concentration in fluid phase, $mol \cdot m^{-3}$

$D$ = adsorbate axial diffusivity, $m^2 \cdot s^{-1}$

$f$ = particle distribution function related to fluid-phase concentration, dimensionless

$k$ = index for lattice (streaming) link, dimensionless

$k_{ads}$ = adsorption kinetic constant, $m^3 \cdot mol^{-1} \cdot s^{-1}$

$k_{des}$ = desorption kinetic constant, $s^{-1}$

$L$ = chromatographic column length, m

Ma = lattice-based Mach number, dimensionless

$N_z$ = index of the last lattice site, dimensionless

$Pe_m$ = lattice-based mass-transfer Peclet number, dimensionless

$P_{ads}$ = adsorption-related parameter, dimensionless

$P_{des}$ = desorption-related parameter, dimensionless

$P_{max}$ = inlet concentration and maximum adsorption capacity parameter, dimensionless

$Q$ = dimensionless adsorbate concentration in solid phase

$q$ = adsorbate concentration in solid phase, $mol \cdot m^{-3}$

$\dot{R}$ = dimensionless adsorbate transfer rate from fluid to solid phase

$\dot{r}$ = adsorbate transfer rate from fluid to solid phase, $mol \cdot m^{-3} \cdot s^{-1}$

$\vec{r}$ = particle position, m

$s$ = particle distribution function related to solid-phase concentration, dimensionless

$t$ = time, s

$\vec{u}$ = particle velocity, $m \cdot s^{-1}$

$\dot{V}$ = volumetric flow rate of the percolating solution, $m^3 \cdot s^{-1}$

$v$ = interstitial velocity of the percolating solution, $m \cdot s^{-1}$

$w$ = weighting factors, dimensionless

$Z$ = dimensionless axial coordinate

$z$ = axial coordinate, m

**Greek Symbols**

$\varepsilon$ = bed porosity, dimensionless

$\tau$ = dimensionless time

$\Omega$ = collision operator, $s^{-1}$

$\omega$ = relaxation parameter, dimensionless

**Subscripts and Superscripts**

eq = equilibrium distribution function

exit = chromatographic column exit

f = fluid phase

in = chromatographic column inlet

$k$ = lattice link (for streaming)

max = maximum adsorption capacity of the chromatographic column

ref = reference value

relax = relaxation time

s = solid phase

$z$ = axial coordinate

0 = central lattice site

1 = downward streaming direction

2 = upward streaming direction

– = superficial velocity (average over a representative elementary volume)

**Abbreviations and Acronyms**

BAC = biospecific affinity chromatography

BGK = Bhatnagar-Gross-Krook approximation

FDM = finite differences method

FEM = finite elements method

FVM = finite volumes method

LBM = lattice Boltzmann method

MD = molecular dynamics

PDE = partial differential equation

1-D = one dimensional

## REFERENCES

[1] Souza-Santos ML. Solid Fuels Combustion and Gasification: Modeling, Simulation, and Equipment Operation. 2nd ed. New York: CRC Press; 2010. Print ISBN 978-1-4200-4749-3, eBook ISBN: 978-1-4200-4750-9.

[2] Diaz MS, Brignole EA. Modeling and optimization of supercritical fluid processes. J Supercrit Fluids 2009; 47: 611-8. http://dx.doi.org/10.1016/j.supflu.2008.09.006

[3] Brannock M, Leslie G, Wang Y, Buetehorn S. Optimising mixing and nutrient removal in membrane bioreactors: CFD modelling and experimental validation. Desalination 2010; 250: 815-8. http://dx.doi.org/10.1016/j.desal.2008.11.048

[4] Głuszcz P, Petera J, Ledakowicz S. Mathematical modeling of the integrated process of mercury bioremediation in the industrial bioreactor. Bioproc Biosyst Eng 2011; 34: 275-85. http://dx.doi.org/10.1007/s00449-010-0469-8

[5] Parco V, Du Toit G, Wentzel M, Ekama G. Biological nutrient removal in membrane bioreactors: denitrification and phosphorus removal kinetics. Water Sci Technol 2007; 56: 125-34. http://dx.doi.org/10.2166/wst.2007.642

[6] Ching CB, Wu YX, Lisso M, Wozny G, Laiblin T, Arlt W. Study of feed temperature control of chromatography using computational fluid dynamics simulation. J Chromatogr A 2002; 945: 117-31. http://dx.doi.org/10.1016/S0021-9673(01)01479-0

[7] Özdural AR, Alkan A, Kerkhof PJAM. Modeling chromatographic columns: non-equilibrium packed-bed adsorption with non-linear adsorption isotherm. J Chromatogr A 2004; 1041: 77-85. http://dx.doi.org/10.1016/j.chroma.2004.05.009

[8] Vidal-Madjar C, Cañada-Cañada F, Jaulmes A, Pantazaki A, Taverna M. Numerical simulation of the chromatographic process for direct ligand-macromolecule binding studies. J Chromatogr A 2005; 1087: 95-103. http://dx.doi.org/10.1016/j.chroma.2005.01.008

[9] Leickt L, Månsson A, Ohlson S. Prediction of affinity and kinetics in biomolecular interactions by affinity chromatography. Anal Biochem 2001; 291: 102-8. http://dx.doi.org/10.1006/abio.2001.5019

[10] Datta AK, Sablani SS. Mathematical modeling techniques in food and bioprocess: an overview. In: Sablani SS, Rahman MS, Datta AK, Mujumdar AR, editors. Handbook of Food and Bioprocess Modeling Techniques. Boca Raton: CRC Press 2007; p. 1-11. ISBN13: 978-0-8247-2671-3.

[11] Norton T, Sun D-W. An overview of CFD applications in the food industry. In: Sun D-W, editor. Computational Fluid Dynamics in Food Processing. Boca Raton: CRC Press 2007; p. 1-41. ISBN 978-0-8493-9286-3.

[12] Puri VM, Anantheswaran RC. The finite-element method in food processing: a review. J Food Eng 1993; 19: 247-74. http://dx.doi.org/10.1016/0260-8774(93)90046-M

[13] Scott G, Richardson P. The application of computational fluid dynamics in the food industry. Trends Food Sci Technol 1997; 8: 119-24. http://dx.doi.org/10.1016/S0924-2244(97)01028-5

[14] Xia B, Sun D-W. Applications of computational fluid dynamics (CFD) in the food industry: a review. Comput Electron Agric 2002; 34: 5-24. http://dx.doi.org/10.1016/S0168-1699(01)00177-6

[15] Wang L, Sun D-W. Recent developments in numerical modelling of heating and cooling processes in the food industry - a review. Trends Food Sci Technol 2003; 14: 408-23. http://dx.doi.org/10.1016/S0924-2244(03)00151-1

[16] Yun J, Lin D-Q, Yao S-J. Predictive modeling of protein adsorption along the bed height by taking into account the axial nonuniform liquid dispersion and particle classification in expanded beds. J Chromatogr A 2005; 1095: 16-26. http://dx.doi.org/10.1016/j.chroma.2005.07.120

[17] Alper HE, Stouch TR. Orientation and diffusion of a drug analogue in biomembranes: Molecular Dynamics simulations. J Phys Chem 1995; 99: 5724-31. http://dx.doi.org/10.1021/j100015a065

[18] Bemporad D, Luttman C, Essex JW. Behaviour of small solutes and large drugs in a lipid bilayer from computer simulation. Biochem Biophys Acta 2005; 1718: 1-21. http://dx.doi.org/10.1016/j.bbamem.2005.07.009

[19] Henneré G, Prognon P, Brion F, Rosilio V, Nicolis I. Molecular Dynamics simulation of a mixed lipid emulsion: influence of the triglycerides on interfacial phospholipid organization. Teochem J Mol Struct 2009; 901: 174-85. http://dx.doi.org/10.1016/j.theochem.2009.01.020

[20] Xiang T-X, Anderson BD. Lipossomal drug transport: a molecular perspective from Molecular Dynamics simulations in lipid bilayers. Adv Drug Deliv Rev 2006; 58: 1357-78. http://dx.doi.org/10.1016/j.addr.2006.09.002

[21] Rothman DH, Zaleski S. Lattice-Gas Cellular Automata: Simple Models of Complex Hydrodynamics. Cambridge: Cambridge University Press; 1997. ISBN-13: 978-0-5216-0760-5. http://dx.doi.org/10.1017/CBO9780511524714

[22] Wolf-Gladrow DA. Lattice-Gas Cellular Automata and Lattice Boltzmann Models: an Introduction. Berlin: Springer; 2000. ISBN: 978-3-540-66973-6. http://dx.doi.org/10.1007/b72010

[23] Succi S. The Lattice Boltzmann Equation for Fluid Dynamics and Beyond. Oxford: Oxford University Press; 2001. ISBN: 978-0-19-850398-9.

[24] McNamara GR, Zanetti G. Use of the Boltzmann equation to simulate lattice-gas automata. Phys Rev Lett 1988; 61: 2332-5. http://dx.doi.org/10.1103/PhysRevLett.61.2332

[25] van der Sman RGM. Lattice Boltzmann simulation of microstructures. In: Sablani SS, Rahman MS, Datta AK, Mujumdar AR, editors. Handbook of Food and Bioprocess Modeling Techniques. Boca Raton: CRC Press 2007; p. 15-39. ISBN13: 978-0-8247-2671-3.

[26] Mantle MD, Bijeljic B, Sederman AJ, Gladden LF. MRI velocimetry and lattice-Boltzmann simulations of viscous flow of a Newtonian liquid through a dual porosity fiber array. Magn Reson Imaging 2001; 19: 527-9. http://dx.doi.org/10.1016/S0730-725X(01)00285-5

[27] Ladd AJC, Verbeg RJ. Lattice-Boltzmann simulations of particle-fluid suspensions. J Stat Phys 2001; 104: 1191-1251. http://dx.doi.org/10.1023/A:1010414013942

[28] Zhang XX, Bengough AG, Deeks LK, Crawford JW, Young IM. A novel three-dimensional lattice Boltzmann model for solute transport in variably saturated porous media. Water Resour Res 2002; 38: 1167-76. http://dx.doi.org/10.1029/2001WR000982

[29] Zhang XX, Ren LJ. Lattice Boltzmann model for agrochemical transport in soils. J Contam Hydrol 2003; 67: 27-42. http://dx.doi.org/10.1016/S0169-7722(03)00086-X

[30] Migliorini C, Qian Y, Chen H, Brown EB, Jain RK, Munn LL. Red blood cells augment leukocyte rolling in a virtual blood vessel. Biophys J 2002; 83: 1834-41. http://dx.doi.org/10.1016/S0006-3495(02)73948-9

[31] Sun C, Migliorini C, Munn LL. Red blood cells initiate leukocyte rolling in postcapillary expansions: a lattice Boltzmann analysis. Biophys J 2003; 85: 208-22. http://dx.doi.org/10.1016/S0006-3495(03)74467-1

[32] Sukop MC, Or D. Lattice Boltzmann method for modeling liquid-vapor interface configurations in porous media. Water Resour Res 2004; 40: W01509. http://dx.doi.org/10.1029/2003WR002333

[33] Agarwal S, Verma N, Mewes D. A lattice Boltzmann model for adsorption breakthrough. Heat Mass Transf 2005; 41: 843-54. http://dx.doi.org/10.1007/s00231-005-0625-x

[34] Schure MR, Maier RS, Kroll DM, Davis HT. Simulation of ordered packed beds in chromatography. J Chromatogr A 2004; 1031: 79-86. http://dx.doi.org/10.1016/j.chroma.2003.12.030

[35] Okiyama DCG, Rabi JA. Lattice-Boltzmann Simulation of Transport Phenomena in Agroindustrial Biosystems. In: Kora AB, editor. Advances in Computational Modeling Research: Theory, Developments and Applications. Hauppauge: Nova Science Publishers 2013; p. 79-104. ISBN: 978-1-62618-065-9.

[36] Golshan-Shirazi S, Guiochon G. Modeling of preparative liquid chromatography. J Chromatogr A 1994; 658: 149-71. http://dx.doi.org/10.1016/0021-9673(94)80013-8

[37] Guiochon G, Golshan-Shirazi S. A retrospective on the solution of the ideal model of chromatography. J Chromatogr A 1994; 658: 173-7. http://dx.doi.org/10.1016/0021-9673(94)80014-6

[38] Chase HA. Prediction of the performance of preparative affinity chromatography. J Chromatogr 1984; 297: 179-202. http://dx.doi.org/10.1016/S0021-9673(01)89041-5

[39] Mendieta-Taboada O, Kamimura ES, Maugeri Filho F. Modelling and simulation of the adsorption of the lipase from *Geotrichum sp* on hydrophobic interactions columns. Biotechnol Lett 2001; 23: 781-6. http://dx.doi.org/10.1023/A:1010302416897

[40] Mohamad AA. Lattice Boltzmann Method: Fundamentals and Engineering Applications with Computer Codes. London: Springer-Verlag; 2011. ISBN: 9780857294548. http://dx.doi.org/10.1007/978-0-85729-455-5

[41] Cowan GH, Gosling IS, Laws JF, Sweetenham WP. Physical and mathematical modeling to aid scale-up of liquid chromatography. J Chromatogr 1986; 363: 37-56. http://dx.doi.org/10.1016/S0021-9673(00)88990-6

[42] Kempe H, Axelsson A, Nilsson B, Zacchi G. Simulation of chromatographic processes applied to separation of proteins. J Chromatogr A 1999; 846: 1-12. http://dx.doi.org/10.1016/S0021-9673(98)01079-6

[43] Sridhar P, Sastri NVS, Modak JM, Mukherjee AK. Mathematical simulation of bioseparation in an affinity packed column. Chem Eng Technol 1994; 17: 422-9. http://dx.doi.org/10.1002/ceat.270170610

[44] Nield DA, Bejan A. Convection in Porous Medium. New York: Springer-Verlag; 1992. ISBN: 0-387-97651-5. http://dx.doi.org/10.1007/978-1-4757-2175-1

[45] Sanchez FJM, del Valle EM, Serrano MAG, Cerro RL. Modeling of monolith supported affinity chromatography. Biotechnol Prog 2004; 20: 811-7. http://dx.doi.org/10.1021/bp034343n

[46] Okiyama DCG, Rabi JA. Dirichlet versus Danckwerts inlet condition for bioaffinity chromatography part 2: comparing results from lattice-Boltzmann simulations. In: Proceedings of the XIX SINAFERM - X SHEB; 2013: Iguassu Falls, Brazil: UFSCar / UNICAMP / UEM / ABEQ; 2013: CD-ROM.

[47] Qian YH, D'Humières D, Lallemand P. Lattice BGK models for Navier-Stokes equation. Europhys Lett 1992; 17: 479-84. http://dx.doi.org/10.1209/0295-5075/17/6/001

[48] Karlin IV, Ansumali S, Frouzakis CE, Chikatamarla SS. Elements of the lattice Boltzmann method I: linear advection equation. Commun Comput Phys 2006; 1: 1-45. Available from: http://65.54.113.26/Publication/7038361/elements-of-the-lattice-boltzmann-method-i-linear-advection-equation.

[49] Maier RS, Bernard RS, Daryl WG. Boundary conditions for the lattice Boltzmann method. Phys Fluids 1996; 8: 1788-1801. http://dx.doi.org/10.1063/1.868961

[50] Rabi JA, Mohamad AA. Simulation of zero-order transport problems using lattice-Boltzmann method: imposition of periodic boundary conditions or suppression of streaming step. In: Proceedings of the 17th Discrete Simulation of Fluids Dynamics; 2008: Florianopolis, Brazil: UFSC; 2008: p. 25.

[51] Patankar SV. Numerical Heat Transfer and Fluid Flow. New York: Hemisphere; 1980. ISBN-13: 978-0891165224.

[52] Rabi JA. Numerical simulation of mass transfer aiming at food processes and bioprocesses in fixed-bed equipment: a comparison between finite-differences and lattice-Boltzmann method. WSEAS Trans Heat Mass Transf 2012; 7: 69-78. Available from: http://www.wseas.org/wseas/cms.action?id=6941.

[53] Kamimura ES, Mediata O, Rodrigues MI, Maugeri Filho F. Studies on lipase-affinity adsorption using response-surface analysis. Biotechnol Appl Biochem 2001; 33: 153-9. http://dx.doi.org/10.1042/BA20000081

Received on 02-02-2015 Accepted on 29-03-2015 Published on 08-04-2015

DOI: http://dx.doi.org/10.6000/1927-3037.2015.04.01.5